Revisiting the Activation Function for Federated Image Classification

Jaewoo Shin, Taehyeon Kim, Se-Young Yun
KAIST AI
Seoul, Korea
{yimsungen5, potter32, yunseyoung}@kaist.ac.kr

Abstract

Federated learning (FL) has become one of the most popular distributed machine learning paradigms; these paradigms enable training on a large corpus of decentralized data that resides on devices. The recent evolution in FL research is mainly credited to the refinements in training procedures by developing the optimization methods. However, there has been little verification of other technical improvements, especially improvements to the activation functions (e.g., ReLU), that are widely used in the conventional centralized approach (i.e., standard data-centric optimization). In this work, we verify the effectiveness of activation functions in various federated settings. We empirically observe that off-the-shelf activation functions that are used in centralized settings exhibit a totally different performance trend than do federated settings. The experimental results demonstrate that HardTanh achieves the best accuracy when severe data heterogeneity or low participation rate is present. We provide a thorough analysis to investigate why the representation powers of activation functions are changed in a federated setting by measuring the similarities in terms of weight parameters and representations. Lastly, we deliver guidelines for selecting activation functions in both a *cross-silo* setting (i.e., a number of clients $\leq$ 20) and a *cross-device* setting (i.e., a number of clients $\geq$ 100). We believe that our work provides benchmark data and intriguing insights for designing models FL models. The code is available at https://github.com/Jaewoo-Shin/FL_ACT.

1 Introduction

Federated learning (FL) has become a common and ubiquitous paradigm for collaborative machine learning techniques [3, 4, 23, 33, 34, 44, 37, 45] because it maintains data privacy. Each client (e.g., mobile devices or the whole business) communicates with the central server by transferring the model but not the data; all local updates are aggregated in a global server-side model. Although a centralized method enhances generalization by employing a large amount of training data, the features of the FL methods appear to differ from those of a centralized method owing to data heterogeneity, client resource capability, and model communication [24, 37, 50].

Most FL studies focus on improving the performance of the global model. To this end, they apply a new regularizer in the optimization algorithm [1, 25, 32, 33, 18, 35, 46, 47, 48, 50, 21, 10, 13]. Recently, there has been an increasing demand for the personalization of models according to the client. Jiang et al. [22] and Fallah et al. [9] attempt to train personalized models for each client with a few rounds of fine-tuning rather than focusing on the performance of a server model. In consideration of system heterogeneity (i.e., clients having different computational and communication capabilities), Avdiukhin et al. [2] mitigate model communication problems by using asynchronous local SGD; Horvath et al. [17] improve accuracy in heterogeneous resource capacity by using different model sizes per client.

36th Conference on Neural Information Processing Systems (NeurIPS 2022).

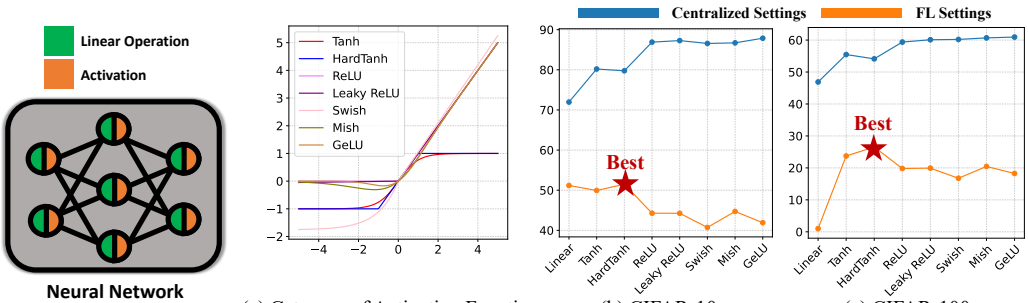

(a) Category of Activation Functions (b) CIFAR-10 (c) CIFAR-100

Figure 1: (a) Plots of different activation functions. (b), (c) Accuracies on CIFAR-10 and CIFAR-100 according to the changes of activation functions, respectively. The blue line indicates the performances of models trained in a single central server. The orange line indicates those of models trained in FL environment where 20 clients participate in the training per round among the total 100 clients. We use a model with four convolution layers and one classifier. Here, 'Linear' indicates the model without any activation function. In one machine centralizing the training data, the more up-to-date activation function used, the better the performance (Blue line). In contrast, interestingly, HardTanh [7] prints the best server accuracy for both CIFAR-10 and CIFAR-100 under heterogeneous scenarios (Orange line). The detailed explanation about activation functions are provided in Appendix A.

Despite the popularity of FL, some options for federated model optimization remain under-explored. Designing FL-familiar training recipes is essential to optimizing model performance, but few studies have attempted to design a new recipe instead of using those intended for a centralized setting. Charles et al. [5] present an empirical analysis of the impact of hyperparameter settings for federated training dynamics from the perspective of a large cohort size. However, FL activation functions [37, 25, 34] have rarely been studied, whereas activation functions play a crucial role in facilitating generalization and convergence. We thus raise the seemingly doubtful question: *Do activation functions that are popular in centralized settings also produce good optima in FL?*

We conduct a pilot experiment to compare performance in centralized settings with performance in FL settings to answer this question. Figure 1 (b) and (c) show the accuracy of neural networks trained under a centralized setting and a FL setting according to the changes in activation functions. A shallow neural network that uses Tanh has better accuracy than ReLU, which is a silver bullet in the centralized deep learning field. The problems mentioned above lead us to the intriguing question:

Do off-the-shelf activation functions intended for a centralized setting also perform appropriately in the FL setting?

In this work, we answer the question with thorough empirical evaluations: *the latest developed activation functions rather degrade the performance of the server as the heterogeneity gets severe.*

Several considerations (e.g., the total number of clients, client participation, heterogeneity) in selecting activation functions may improve significantly. Combining considerations may further boost the model accuracy. We experiment with various activation functions, including widely-used and rarely-used functions in the centralized setting, in various environments based on CIFAR-10 and CIFAR-100. The experiments identify an interesting phenomenon in FL in which applying activation functions like ReLU in stacked convolutional layers demonstrates low accuracy owing to the shape of the function. We also provide an analysis of the representation power according to the changes in activation functions for federated image classification. Our key contributions are summarized as follows:

- We provide guidelines for selecting activation functions in FL. FL has the following special considerations: number of clients, participation ratio, and non-IIDness. We provide guidelines for *cross-silo* settings (i.e., for a number of clients ≤ 20) and *cross-device* settings (i.e., for a number of clients ≥ 100); the suitable activation function depends on the situation.
- We provide an explanation for the performance degradetion (i.e., for the performance difference between centralized settings and FL settings) of activation functions, that are the preferred in a centralized setting. Specifically, we measure the similarities in the manner of weight parameters and representations.
- We empirically show that the HardTanh activation function [7] leads to a better optimum do other activation functions such as ReLU [39], Leaky ReLU [36], and GeLU [16] for severe

Table 1: Accuracy of centralized and FL settings in two datasets. Centralized settings train one server model using all training data and FL settings train 100 clients with heterogeneous data. We use $R = 0.2$, and $\alpha = 0.1$.

Activation Function	CIFAR-10		CIFAR-100	
	Centralized Setting	FL setting	Centralized Setting	FL Setting
Linear	73.74±1.54	10.00	46.52±0.31	28.39
Tanh	81.00±0.89	52.58	55.39±0.24	30.75
HardTanh	80.64±0.77	**54.43**	54.31±0.46	**31.76**
ReLU	87.01±0.11	48.37	59.75±0.33	23.99
Leaky ReLU	87.30±0.03	48.34	60.28±0.22	24.04
Swish	86.50±0.08	46.16	60.02±0.47	21.55
Mish	86.38±0.29	50.02	60.67±0.03	24.98
GeLU	**87.77±0.11**	47.46	**61.34±0.35**	23.26

non-IID setting, a low participation rate, and with a large number of clients, and we provide benchmark data for activation functions in FL.

2 Related Work

This work is related to activation functions in neural networks, and FL methods. For details, refer to Appendix A.

3 Experiments

In this section, we compare several activation functions. We categorize the activation functions into two groups: (1) ReLU, Leaky ReLU, Swish, Mish, and GeLU as recent SOTA activation functions that are widely used in centralized settings; and (2) Tanh and HardTanh as Tanh-like activation functions that are not widely used in centralized settings.

3.1 Experimental Setup

Dataset and Heterogenous Settings. We use two benchmark datasets: CIFAR-10 and CIFAR-100 [29]. We provide the descriptions of the datasets in Appendix B. To randomize the heterogeneous data, we assume that all client training data use class labels according to an independent categorical distribution for N classes parameterized by the vector q:

$$q_i \geq 0,\ i \in [1, N] \quad \text{and} \quad \sum_{i \in [1,N]} q_i = 1$$

For the heterogeneous distribution, the *Dirichlet distribution* [18, 48], $q \sim \mathrm{Dir}(\boldsymbol{\alpha})$ is used, where $\boldsymbol{\alpha}$ is an N-length concentration vector having all elements $\alpha > 0$, that is, the prior distribution for N classes controls the heterogeneity of clients.

Models. Our study focuses on compact models that are realistically possible in FL. Therefore, we use a simple `ConvNet` having four convolutional layers and one classifier; `ConvNet4` refers to `ConvNet` with four convolutional layers. The first convolution layer has 64 kernels, and deeper layers have a larger number of kernels [40]. For additional models, which have a shortcut and batch normalization layer, we use `Resnet20`, `Resnet32`, `Resnet44` [15], and `MobileNetv2` [43].

Training Details. In this study, we conduct numerical experiments by varying the number of clients N, the client participation ratio R, and the Dirichlet distribution constant α. We mainly exhibit the training of `ConvNet4` on heterogeneously distributed CIFAR-10 by modifying R and α. In the captions, we explain each N, R, and α value. The details are explained in Appendix B.

3.2 Comparative Experiments on the Changes in Activation Functions

Table 1 shows the result of both centralized and FL settings using CIFAR-10 and CIFAR-100 as the datasets. In centralized settings, GeLU shows the best performance, and other recent SOTA activation functions surpass the Tanh-like activation functions. However, in FL settings, the activation functions show a significantly different tendency. HardTanh achieves the highest accuracy. Furthermore, the recent SOTA activation functions show lower accuracy than Linear using CIFAR-100 as the dataset.

Table 2: Server accuracy of `ConvNet4` with four different Dirichlet constant values α (0.01, 0.1, 1, 10). We use $N = 100$ and $N = 20$ with $R = 0.2$.

Activation Function	$N = 100$				$N = 20$			
	$\alpha = 10$	$\alpha = 1$	$\alpha = 0.1$	$\alpha = 0.01$	$\alpha = 10$	$\alpha = 1$	$\alpha = 0.1$	$\alpha = 0.01$
Linear	62.48	62.43	10.00	10.00	66.48	66.48	63.54	10.00
Tanh	64.49	64.14	52.58	29.50	70.22	69.55	65.97	27.64
HardTanh	**65.27**	**65.40**	**54.43**	30.09	70.53	70.01	**66.53**	28.92
ReLU	57.80	56.23	48.37	34.03	75.59	74.21	63.39	34.70
Leaky ReLU	57.85	56.16	48.34	33.92	75.36	74.23	63.67	35.15
Swish	52.62	51.48	46.16	35.65	72.58	71.58	64.57	36.93
Mish	57.30	55.08	50.02	**38.94**	73.69	72.95	66.47	**37.89**
GeLU	55.59	54.34	47.46	36.09	**75.68**	**74.41**	65.62	37.77

Table 3: Server accuracy of `ConvNet4` with four different participation ratios R (0.1, 0.2, 0.3, 0.4). We use $N = 100$ and $N = 20$ with $\alpha = 0.1$.

Activation Function	$N = 100$				$N = 20$			
	$R = 0.4$	$R = 0.3$	$R = 0.2$	$R = 0.1$	$R = 0.4$	$R = 0.3$	$R = 0.2$	$R = 0.1$
Linear	10.00	10.00	10.00	10.00	65.85	66.12	63.54	58.36
Tanh	**62.61**	61.79	52.58	**46.61**	69.22	67.75	65.97	**62.67**
HardTanh	59.45	**61.75**	**54.43**	41.90	69.25	68.80	**66.53**	43.96
ReLU	53.26	50.67	48.37	41.95	71.96	70.17	63.39	54.47
Leaky ReLU	53.17	50.76	48.34	42.05	66.12	**70.22**	63.67	54.46
Swish	51.72	49.45	46.16	40.00	70.36	67.99	64.57	53.74
Mish	56.67	52.80	50.02	43.37	71.30	69.34	66.47	60.38
GeLU	53.35	50.61	47.46	41.50	**72.32**	70.10	65.62	54.05

Activation functions have different accuracy drop; only recent SOTA activation functions have an accuracy drop near 40, while HardTanh and Tanh have 26.21 and 28.42 at CIFAR-10. As a result, we can find that the most popular activation function, ReLU (as well as recent SOTA activation functions), does not show outstanding performance in an FL setting.

3.3 Strategies for Selecting Activation Functions in FL

This section presents the experimental results and guidelines for selecting the activation functions for various FL settings. FL settings have various environmental limitations relative to centralized settings. It has additional components to consider, such as the number of clients, IID-ness, and the participation ratio.

Number of Clients. In different FL strategies, the number of clients varies. A *cross-silo* setting uses fewer than 20 clients, and a *cross-device* setting use more than 100 clients. As the number of clients differs, the drop in accuracy caused by the activation functions varies. The $\alpha = 0.1$ columns of Table 2 lists the accuracy for different client numbers. As the number of clients decreases, the overall drop in accuracy decreases. For both numbers of clients, HardTanh achieves the highest accuracy. However, the accuracy difference between the recent SOTA activation functions and Tanh-like activation functions is larger for 100 clients. Considering the observations for the number of clients, we hypothesize that as the number of clients increases, recent SOTA activation functions are increasingly affected and show a more significant accuracy drop.

IID-ness. With the Dirichlet distribution parameter α, we can control the IID-ness: a larger value of α indicates higher IID-ness (lower heterogeneity). Table 2 presents the accuracy for different different values of α. In most cases, HardTanh shows the highest accuracy. For 100 clients, at lower IID-ness the accuracy of the Tanh-like activation functions surpasses the accuracy of the recent SOTA activation functions with larger accuracy gap. For 20 clients, the recent SOTA activation functions surpass the Tanh-like activation functions at high IID-ness. Activation's shape cause severe accuracy drop of the recent SOTA activations with low IID-ness, which we discuss at section 4. The low accuracy of the Tanh-like activation functions at $\alpha = 0.01$ occurs due to tough training settings and the Tanh-like activation functions fail to find the optimum, such as Linear.

Participation Ratio. The participation of clients is limited in FL depending on the environment. In a *cross-silo* setting, high participation may be possible, whereas only limited participation is available in a the *cross-device* setting. Table 3 shows the accuracy in FL settings for four different values of the

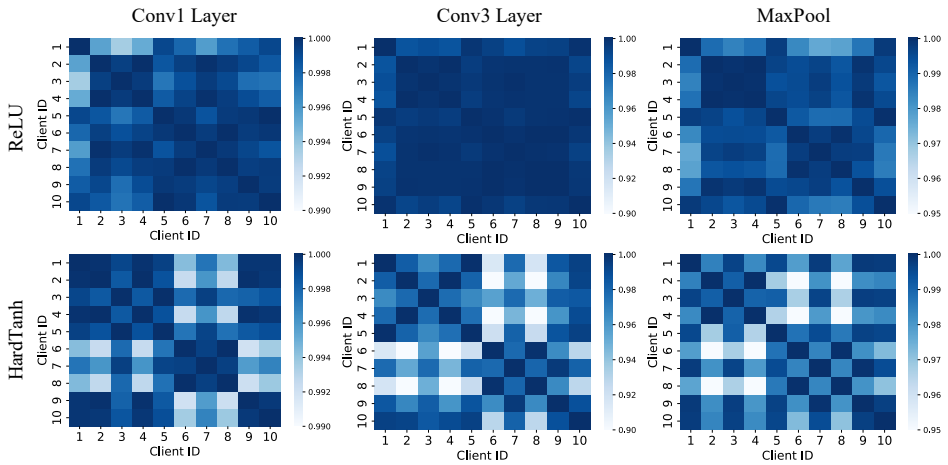

Figure 2: CKA similarity between 10 client using test images of CIFAR-10. Each client's model is the model before $100th$ aggregation. We use $N = 100$ with $R = 1.0$ and $\alpha = 0.1$ for training. We calculate the CKA similarity using features passing through each layer and its activation function.

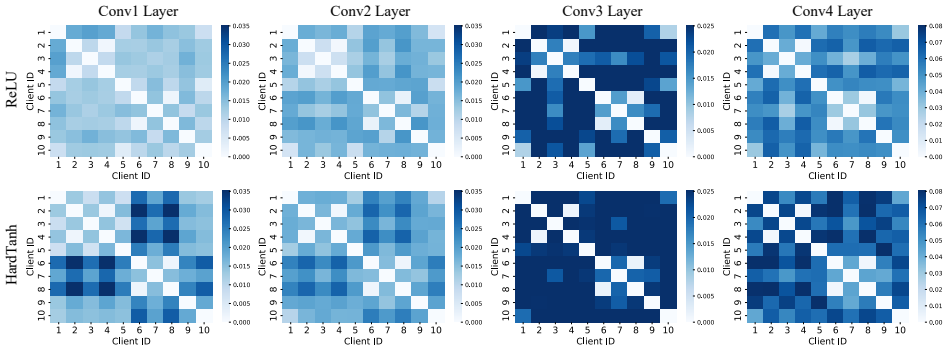

Figure 3: Weight difference between 10 client selected in Figure 2. We calculate the weight difference by subtracting each client's weight from the same layer and normalizing it with L_2norm.

participation ratio. For 100 clients, the Tanh-like activation functions achieve the highest accuracy. With 20 clients, however, there is a noticeably larger accuracy drop as participation decreases for the most recent SOTA activation functions. With higher client participation, *client drift* [25, 26, 42] reduces, and the influence of the activation function's shape of the recent SOTA activation functions drops and occur smaller accuracy.

Different FL settings components affect accuracy when different activation functions are used, according to the observations above. The number of clients is the most dominant component, and it interacts with the influence of other components when a small number of clients is used. Therefore, the Tanh-like activation functions are favorable for a large number of clients, such as in a *cross-device* setting. For a *cross-silo* setting, with low data IID-ness, and a low ratio of client participation the Tanh-like activation functions are preferred. Conversely, the recent SOTA activation functions are preferred for a *cross-silo* setting, with high data IID-ness, and high ratio of client participation.

3.4 Additional Experiment

Additional experiments with different FL method and models showed a similar tendency, where Tanh-like activation functions surpassed recent SOTA activation functions as observed above. We chose FedProx as the additional FL method and `Resnet20`, `Resnet32`, `Resnet44`, and `MobileNetv2` as the additional models. For details of the experimental results, refer to Appendix C.

4 Analysis

We present thorough investigations on model behavior and the changes in representation during the local training to answer this question: *do recent SOTA activation functions have a disadvantage in FL settings?*

4.1 Investigation of Weight Parameters and Latent Representations

The activation function selects important features to pass through each layer, and the model is trained using these features. The number of selected features varies according to the shape of an activation function. In a conventional centralized setting, a single model can access all the data and select optimal training features. However, in an FL setting, each client can only access a portion of the data, which is partitioned in the non-IID condition, and each client trains its model to select features that are important to itself. This results in a phenomenon known as *client drift*. During the FL aggregation step, a problem arises where important features for the global optimum cannot be selected due to client drift. This phenomenon appears to be severe when the recent SOTA activation functions are used. Due to the shape of their activation functions, the excluded features are greater in number than for Tanh-like activation functions, and a severe accuracy drop occurs. Figure 5 (a) in Appendix C shows the feature distribution after the first convolution layer. The recent SOTA activation functions exclude more feature and have a high density near 0. The empirical results in section 3 show that for a large number of clients and a small client participation ratio, the client drift increases, and the accuracy drop for recent SOTA activation functions is maximal.

This can be simply summarized by saying that, the number of excluded features varies due to the different shapes of the activation functions, and as an activation function excludes more feature values, the drop in accuracy increases. Recent SOTA activation functions tend to exclude features smaller than 0. Tanh-like activation functions, on the other hand, exclude features that are smaller than -1 and larger than 1. Tanh-like activation functions have low sensitivity about the accuracy drop in the FL aggregation step because they exclude a much smaller number of features than do recent SOTA activation functions. Additionally, HardTanh and Tanh show better accuracy than Linear in most situations due to their existence of non-linearity. Figure 5 (b) in Appendix C shows the accuracy in FL settings for different versions of `ConvNet`, which have different numbers of convolutional layers. Deeper models exclude more features, and as a result, `ConvNet` used with recent SOTA activation functions shows a significant drop in accuracy.

To observe how the activation function affects `ConvNet4`, we perform two additional experimental studies on heterogeneous local models. For simplicity, we look at 10 clients out of a total 100. First, we perform Centered Kernel Alignment (CKA) [28] to measure the similarity of the output features between different clients. Each client trains the server model for 5 epochs with their own non-IID data. In Figure 2, ReLU has a higher CKA similarity than HardTanh in every layer. Because feature selection fails for the server model, as indicated above, ConvNet4 with ReLU has a smaller feature change than does HardTanh, which indicates a lower learning ability. Second, we calculate the weight differential to check how similar other clients weights are. Figure 3 reveals that ConvNet4 with ReLU has a smaller weight difference in each layer than does HardTanh, which also indicates ReLU has a limited learning ability.

4.2 Analysis of Landscape

To check if each activation functions reaches the global optimum, we visualize the 2-D landscape of Tanh, HardTanh, ReLU, and Leaky ReLU in Appendix D. Figure 5 shows the 2-D landscape of each activation function. It seems that ReLU and Leaky ReLU fails to approach to the global optimum. In contrast, Tanh and HardTanh succeed in reaching the global optimum. Furthermore, ReLU and Leaky ReLU has steep slope in their landscape where Tanh and HardTanh does not.

These findings suggest that the sensitivity of the activation functions in the FL aggregation step, where the accuracy drop occurs, is indicated by the shape of the activation functions. The accuracy drop increases as the number of features excluded by an activation function increases, and it reaches a maximum with severe client drift; a large number of clients, a low client participation ratio, and high heterogeneity.

5 Conclusion

This study clarifies that the drop in accuracy varies according to the activation function in FL. Our key finding is that the accuracy of the recent SOTA activation functions drops in an FL setting due to the shape of the functions, and HardTanh outperforms other activation functions in most environments. Additionally, we provide guidelines and benchmark data for selecting activation functions in various FL settings. We believe that further research is needed to find the silver bullet of activation function in an FL setting, which our paper did not address, and that our work will inspire others.

Acknowledgement

This work was supported by Institute of Information & communications Technology Planning & Evaluation (IITP) grant funded by Korea government (MSIT) [No. 2021-0-00907, Development of Adaptive and Lightweight Edge-Collaborative Analysis Technology for Enabling Proactively Immediate Response and Rapid Learning, 90%] and [No. 2019-0-00075, Artificial Intelligence Graduate School Program (KAIST), 10%].

References

[1] Durmus Alp Emre Acar, Yue Zhao, Ramon Matas Navarro, Matthew Mattina, Paul N Whatmough, and Venkatesh Saligrama. Federated learning based on dynamic regularization. *arXiv preprint arXiv:2111.04263*, 2021.

[2] Dmitrii Avdiukhin and Shiva Kasiviswanathan. Federated learning under arbitrary communication patterns. In *International Conference on Machine Learning*, pages 425–435. PMLR, 2021.

[3] Keith Bonawitz, Hubert Eichner, Wolfgang Grieskamp, Dzmitry Huba, Alex Ingerman, Vladimir Ivanov, Chloe Kiddon, Jakub Konečnỳ, Stefano Mazzocchi, H Brendan McMahan, et al. Towards federated learning at scale: System design. *arXiv preprint arXiv:1902.01046*, 2019.

[4] Sebastian Caldas, Sai Meher Karthik Duddu, Peter Wu, Tian Li, Jakub Konečnỳ, H Brendan McMahan, Virginia Smith, and Ameet Talwalkar. Leaf: A benchmark for federated settings. *arXiv preprint arXiv:1812.01097*, 2018.

[5] Zachary Charles, Zachary Garrett, Zhouyuan Huo, Sergei Shmulyian, and Virginia Smith. On large-cohort training for federated learning. *arXiv preprint arXiv:2106.07820*, 2021.

[6] Djork-Arné Clevert, Thomas Unterthiner, and Sepp Hochreiter. Fast and accurate deep network learning by exponential linear units (elus). *arXiv preprint arXiv:1511.07289*, 2015.

[7] Ronan Collobert, Jason Weston, Léon Bottou, Michael Karlen, Koray Kavukcuoglu, and Pavel Kuksa. Natural language processing (almost) from scratch. *Journal of machine learning research*, 12(ARTICLE):2493–2537, 2011.

[8] Stefan Elfwing, Eiji Uchibe, and Kenji Doya. Sigmoid-weighted linear units for neural network function approximation in reinforcement learning. *Neural Networks*, 107:3–11, 2018.

[9] Alireza Fallah, Aryan Mokhtari, and Asuman Ozdaglar. Personalized federated learning: A meta-learning approach. *arXiv preprint arXiv:2002.07948*, 2020.

[10] Jack Goetz and Ambuj Tewari. Federated learning via synthetic data. *arXiv preprint arXiv:2008.04489*, 2020.

[11] Ian Goodfellow, David Warde-Farley, Mehdi Mirza, Aaron Courville, and Yoshua Bengio. Maxout networks. In *International conference on machine learning*, pages 1319–1327. PMLR, 2013.

[12] Richard HR Hahnloser, Rahul Sarpeshkar, Misha A Mahowald, Rodney J Douglas, and H Sebastian Seung. Digital selection and analogue amplification coexist in a cortex-inspired silicon circuit. *Nature*, 405(6789):947–951, 2000.

[13] Weituo Hao, Mostafa El-Khamy, Jungwon Lee, Jianyi Zhang, Kevin J Liang, Changyou Chen, and Lawrence Carin Duke. Towards fair federated learning with zero-shot data augmentation. In *Proceedings of the IEEE/CVF Conference on Computer Vision and Pattern Recognition*, pages 3310–3319, 2021.

[14] Kaiming He, Xiangyu Zhang, Shaoqing Ren, and Jian Sun. Delving deep into rectifiers: Surpassing human-level performance on imagenet classification. In *Proceedings of the IEEE international conference on computer vision*, pages 1026–1034, 2015.

[15] Kaiming He, Xiangyu Zhang, Shaoqing Ren, and Jian Sun. Deep residual learning for image recognition. In *Proceedings of the IEEE conference on computer vision and pattern recognition*, pages 770–778, 2016.

[16] Dan Hendrycks and Kevin Gimpel. Gaussian error linear units (gelus). *arXiv preprint arXiv:1606.08415*, 2016.

[17] Samuel Horvath, Stefanos Laskaridis, Mario Almeida, Ilias Leontiadis, Stylianos I Venieris, and Nicholas D Lane. Fjord: Fair and accurate federated learning under heterogeneous targets with ordered dropout. *arXiv preprint arXiv:2102.13451*, 2021.

[18] Tzu-Ming Harry Hsu, Hang Qi, and Matthew Brown. Measuring the effects of non-identical data distribution for federated visual classification. *arXiv preprint arXiv:1909.06335*, 2019.

[19] Hidenori Ide and Takio Kurita. Improvement of learning for cnn with relu activation by sparse regularization. In *2017 International Joint Conference on Neural Networks (IJCNN)*, pages 2684–2691. IEEE, 2017.

[20] Kevin Jarrett, Koray Kavukcuoglu, Marc'Aurelio Ranzato, and Yann LeCun. What is the best multi-stage architecture for object recognition? In *2009 IEEE 12th international conference on computer vision*, pages 2146–2153. IEEE, 2009.

[21] Eunjeong Jeong, Seungeun Oh, Hyesung Kim, Jihong Park, Mehdi Bennis, and Seong-Lyun Kim. Communication-efficient on-device machine learning: Federated distillation and augmentation under non-iid private data. *arXiv preprint arXiv:1811.11479*, 2018.

[22] Yihan Jiang, Jakub Konečnỳ, Keith Rush, and Sreeram Kannan. Improving federated learning personalization via model agnostic meta learning. *arXiv preprint arXiv:1909.12488*, 2019.

[23] Peter Kairouz, H Brendan McMahan, Brendan Avent, Aurélien Bellet, Mehdi Bennis, Arjun Nitin Bhagoji, Kallista Bonawitz, Zachary Charles, Graham Cormode, Rachel Cummings, et al. Advances and open problems in federated learning. *arXiv preprint arXiv:1912.04977*, 2019.

[24] Peter Kairouz, H Brendan McMahan, Brendan Avent, Aurélien Bellet, Mehdi Bennis, Arjun Nitin Bhagoji, Kallista Bonawitz, Zachary Charles, Graham Cormode, Rachel Cummings, et al. Advances and open problems in federated learning. *Foundations and Trends® in Machine Learning*, 14(1–2):1–210, 2021.

[25] Sai Praneeth Karimireddy, Satyen Kale, Mehryar Mohri, Sashank Reddi, Sebastian Stich, and Ananda Theertha Suresh. Scaffold: Stochastic controlled averaging for federated learning. In *International Conference on Machine Learning*, pages 5132–5143. PMLR, 2020.

[26] Ahmed Khaled, Konstantin Mishchenko, and Peter Richtárik. First analysis of local gd on heterogeneous data. *arXiv preprint arXiv:1909.04715*, 2019.

[27] Günter Klambauer, Thomas Unterthiner, Andreas Mayr, and Sepp Hochreiter. Self-normalizing neural networks. In *Proceedings of the 31st international conference on neural information processing systems*, pages 972–981, 2017.

[28] Simon Kornblith, Mohammad Norouzi, Honglak Lee, and Geoffrey Hinton. Similarity of neural network representations revisited. In *International Conference on Machine Learning*, pages 3519–3529. PMLR, 2019.

[29] Alex Krizhevsky, Geoffrey Hinton, et al. Learning multiple layers of features from tiny images. 2009.

[30] Alex Krizhevsky, Ilya Sutskever, and Geoffrey E Hinton. Imagenet classification with deep convolutional neural networks. *Advances in neural information processing systems*, 25:1097–1105, 2012.

[31] Yann LeCun et al. Lenet-5, convolutional neural networks. *URL: http://yann. lecun. com/exdb/lenet*, 20(5):14, 2015.

[32] Qinbin Li, Bingsheng He, and Dawn Song. Model-contrastive federated learning. In *Proceedings of the IEEE/CVF Conference on Computer Vision and Pattern Recognition*, pages 10713–10722, 2021.

[33] Tian Li, Anit Kumar Sahu, Manzil Zaheer, Maziar Sanjabi, Ameet Talwalkar, and Virginia Smith. Federated optimization in heterogeneous networks. *Proceedings of Machine Learning and Systems*, 2:429–450, 2020.

[34] Xiang Li, Kaixuan Huang, Wenhao Yang, Shusen Wang, and Zhihua Zhang. On the convergence of fedavg on non-iid data. *arXiv preprint arXiv:1907.02189*, 2019.

[35] Tao Lin, Lingjing Kong, Sebastian U Stich, and Martin Jaggi. Ensemble distillation for robust model fusion in federated learning. *Advances in Neural Information Processing Systems*, 33: 2351–2363, 2020.

[36] Andrew L Maas, Awni Y Hannun, Andrew Y Ng, et al. Rectifier nonlinearities improve neural network acoustic models. In *Proc. icml*, volume 30, page 3. Citeseer, 2013.

[37] Brendan McMahan, Eider Moore, Daniel Ramage, Seth Hampson, and Blaise Aguera y Arcas. Communication-efficient learning of deep networks from decentralized data. In *Artificial intelligence and statistics*, pages 1273–1282. PMLR, 2017.

[38] Diganta Misra. Mish: A self regularized non-monotonic activation function. *arXiv preprint arXiv:1908.08681*, 2019.

[39] Vinod Nair and Geoffrey E Hinton. Rectified linear units improve restricted boltzmann machines. In *Icml*, 2010.

[40] Keiron O'Shea and Ryan Nash. An introduction to convolutional neural networks. *arXiv preprint arXiv:1511.08458*, 2015.

[41] Prajit Ramachandran, Barret Zoph, and Quoc V Le. Searching for activation functions. *arXiv preprint arXiv:1710.05941*, 2017.

[42] Sashank Reddi, Zachary Charles, Manzil Zaheer, Zachary Garrett, Keith Rush, Jakub Konečnỳ, Sanjiv Kumar, and H Brendan McMahan. Adaptive federated optimization. *arXiv preprint arXiv:2003.00295*, 2020.

[43] Mark Sandler, Andrew Howard, Menglong Zhu, Andrey Zhmoginov, and Liang-Chieh Chen. Mobilenetv2: Inverted residuals and linear bottlenecks. In *Proceedings of the IEEE conference on computer vision and pattern recognition*, pages 4510–4520, 2018.

[44] Reza Shokri and Vitaly Shmatikov. Privacy-preserving deep learning. In *Proceedings of the 22nd ACM SIGSAC conference on computer and communications security*, pages 1310–1321, 2015.

[45] Virginia Smith, Chao-Kai Chiang, Maziar Sanjabi, and Ameet Talwalkar. Federated multi-task learning. *arXiv preprint arXiv:1705.10467*, 2017.

[46] Hongyi Wang, Mikhail Yurochkin, Yuekai Sun, Dimitris Papailiopoulos, and Yasaman Khazaeni. Federated learning with matched averaging. *arXiv preprint arXiv:2002.06440*, 2020.

[47] Jianyu Wang, Qinghua Liu, Hao Liang, Gauri Joshi, and H Vincent Poor. Tackling the objective inconsistency problem in heterogeneous federated optimization. *Advances in neural information processing systems*, 33:7611–7623, 2020.

[48] Mikhail Yurochkin, Mayank Agarwal, Soumya Ghosh, Kristjan Greenewald, Nghia Hoang, and Yasaman Khazaeni. Bayesian nonparametric federated learning of neural networks. In *International Conference on Machine Learning*, pages 7252–7261. PMLR, 2019.

[49] Jie Zhang, Song Guo, Xiaosong Ma, Haozhao Wang, Wenchao Xu, and Feijie Wu. Parameterized knowledge transfer for personalized federated learning. *Advances in Neural Information Processing Systems*, 34, 2021.

[50] Yue Zhao, Meng Li, Liangzhen Lai, Naveen Suda, Damon Civin, and Vikas Chandra. Federated learning with non-iid data. *arXiv preprint arXiv:1806.00582*, 2018.

Appendix

A Related Work

A.1 Activation Functions in Neural Networks

In deep neural networks, using activation functions is a ubiquitous technique for learning non-linear latent representations; an input signal is transformed into the non-linear output centered on zero. Recent evolution occurs along with the enhancement of representation power and the efficiency of computational costs. In the experiment, we use the following non-linear activation functions:

Tanh. The equation of Tanh is:

$$\tanh(x) = \frac{e^x - e^{-x}}{e^x + e^{-x}}$$

It is known that it is zero-centered, but computationally expensive and causes vanishing gradient problems as neural networks become deeper.

HardTanh. It is another variant of the hyperbolic tangent function, which represents computationally more efficient form of tanh:

$$\mathrm{HTanh}(x) = \min(1, \max(-1, x))$$

ReLU. The equation of ReLU [12, 20, 39] is:

$$\mathrm{ReLU}(x) = \max(0, x)$$

ReLU is the abbreviation of *Rectified Linear Unit*, a modified linear function. When the input value of ReLU is negative, the gradient of its output value is zero; the model does not learn. ReLU has shown great performance with Convolutional Neural Networks (CNN) [30, 31]. Since ReLU is computationally cheap, it is still commonly used regardless of numerous attempts to replace it [36, 11, 14, 6, 27, 8].

Leaky ReLU. The equation of Leaky ReLU [36] is:

$$\mathrm{LReLU}(x) = \max(0.01x, x)$$

This function was created to solve the *Dying ReLU* problem in ReLU. It is ReLU multiplied by a tiny constant on the negative part. Due to the small range, the graphs are drawn almost similarly with ReLU.

Swish. The equation of Swish [41] is:

$$\mathrm{Swish}(x) = x \cdot sigmoid(x)$$

This function shows better accuracy than ReLU in deep neural networks regardless of batch size.

Mish. The equation of Mish [38] is:

$$\mathrm{Mish}(x) = x \cdot tanh(ln(1 + e^x)))$$

This function has the characteristic of allowing gradients to flow better than the Relu Zero Bound because it allows some negative numbers.

GeLU. The equation of GeLU [16] is:

$$\mathrm{GeLU}(x) = x \cdot \frac{1}{2}[1 + tanh[\sqrt{2\pi}(x + 0.044715x^3)]]$$

This function is widespread on BERT, GPT, VIT models. GeLU is derived by combining the characteristics of dropout, zoneout, and ReLU.

Activation functions have been devised for the *gradient exploding/vanishing* issues; the magnitude of gradients becomes either near zero or infinite during backward propagation. A general choice for activation functions is ReLU which raises significantly cheap computational costs. Still, it is not differentiable at zero as well as causes significant dying neurons forgetting the information during propagation. Recently, some works [41, 38] lead to more smooth optima by designing self-regularized gradients. On the other hand, these studies are based on centralized settings, whereas those based on FL settings are badlands. Details of activation functions are explained in Appendix B.

A.2 Federated Learning Methods

Federated optimization methods manage to handle multiple clients without collecting data, and they use server weights from a central server to coordinate the global model across the network. In particular, these methods aim to minimize the following objective function:

$$\min_{w} f(w) \quad \text{where} \quad f(w) = \frac{1}{N}\sum_{k=1}^{N} f^{(k)}(w) \tag{1}$$

where $f^{(k)}$ is the loss function based on the client k. N is the total number of clients. At each round $K \ll N$ clients are selected from the total devices. The selected clients run each local model using SGD for E number of local epochs and finally aggregate the selected models at the server model.

In the FL environment, the oracle of a global model can be drifted by optimizing the local clients because the statistical data heterogeneity causes different local optimums widely apart from each other. It is called *Client drift* [25, 26, 42] which indicates the inconsistency among each optimum. Recently, some works prevent *Client drift* designing aggregation methods; Wang et al. [47] present a method of normalized averaging that removes objective inconsistency, and Zhang et al. [49] propose a training algorithm for group knowledge transfer, which allows each client to keep a personalized prediction on the server to assist the local training of others.

Federated Averaging (FedAvg [37]) uses the local server for stochastic gradient descent (SGD) locally for E number of epochs. As a result, the selected client resulting k's weight is updated as w_k. At each round, to aggregate the local client models, FedAvg sums and averages for the server model parameters formulated as:

$$w^t = \frac{1}{K}\sum_{k \in S_t} w_k^t \tag{2}$$

where w^t is the server weight of the t-th round, w_i^t is the client k's model after local training using w^{t-1}, and S_t is the client set. McMahan et al. [37] empirically shows the significance of tuning the hyperparameters in FL training additionally, we present that with respect to the architectural and operational side.

A.3 Algorithms of Federated Learning Methods

We use both FedAvg and FedProx for federated learning methods. Algorithm 1 shows the algorithm of FedAvg and Algorithm 2 shows the algorithm of FedProx. FedProx is similar to FedAvg in that it selects a selection of clients at each round, performs local training, and then averages client's weight to generate a global update. However, the difference between FedAvg and FedProx is shown in line 6. For local training, FedAvg trains each client's model using SGD with its local data whereas FedProx, trains each client with additional proximal term, $\frac{\mu}{2}\left\|w - w^t\right\|^2$. Using the proximal term which contributes to the method's stability by efficiently reducing the impact of variable modifications.

Algorithm 1 Federated Averaging (FedAvg)

1: **Input:** $K, T, \eta, E, w^0, N, k \in [1, \cdots, N]$
2: **for** $t = 0, \cdots, T-1$ **do**
3: Server selects a subset S_t randomly which includes number of K devices
4: Server send w^t to all selected devices
5: **for** $i = 0, \cdots, E-1$ **do**
6: Selected device $k \in S_t$ updates their local weight w_k^{t+1} using SGD with step-size η
7: **end for**
8: Selected device $k \in S_t$ sends their local weight w_k^{t+1} back to the server
9: Server aggregates the local weights, w_k^{t+1}, and gets new server weight $w^{t+1} = \frac{1}{K}\sum_{k \in S_t} w_k^t$
10: **end for**

Algorithm 2 FedProx

Input: K, T, η, μ, E, w^0, N, $k \in [1, \cdots, N]$
for $t = 0, \cdots, T-1$ **do**
  Server selects a subset S_t randomly which includes number of K devices
  Server send w^t to all selected devices
  for $i = 0, \cdots, E-1$ **do**
    Selected device $k \in S_t$ updates their local weight $w_k^{t+1} \approx \underset{w}{min} h^{(k)}(w; w^t) = f^{(k)}(w) + \frac{\mu}{2} \|w - w^t\|^2$ with step-size η
  end for
  Selected device $k \in S_t$ sends their local weight w_k^{t+1} back to the server
  Server aggregates the local weights, w_k^{t+1}, and gets new server weight $w^{t+1} = \frac{1}{K} \sum_{k \in S_t} w_k^t$
end for

B Implementation Details

B.1 Model Architecture

Figure 4 shows `ConvNet` with five different depth (3,4,5,6, and 7). Each version of `ConvNet` has convolution layer corresponding to the number after the model (e.g., `ConvNet3` has three convolution layers and `ConvNet7` has seven convolution layers). The details of each convolution layer is shown in Table 4. `ConvNet` with different depth use convolution layers sequentially from the top in Table 4 (e.g., `ConvNet3` use Conv1, Conv2, Conv3 whereas, `ConvNet7` use Conv1, Conv2, Conv3, Conv4, Conv5, Conv6, and Conv7).

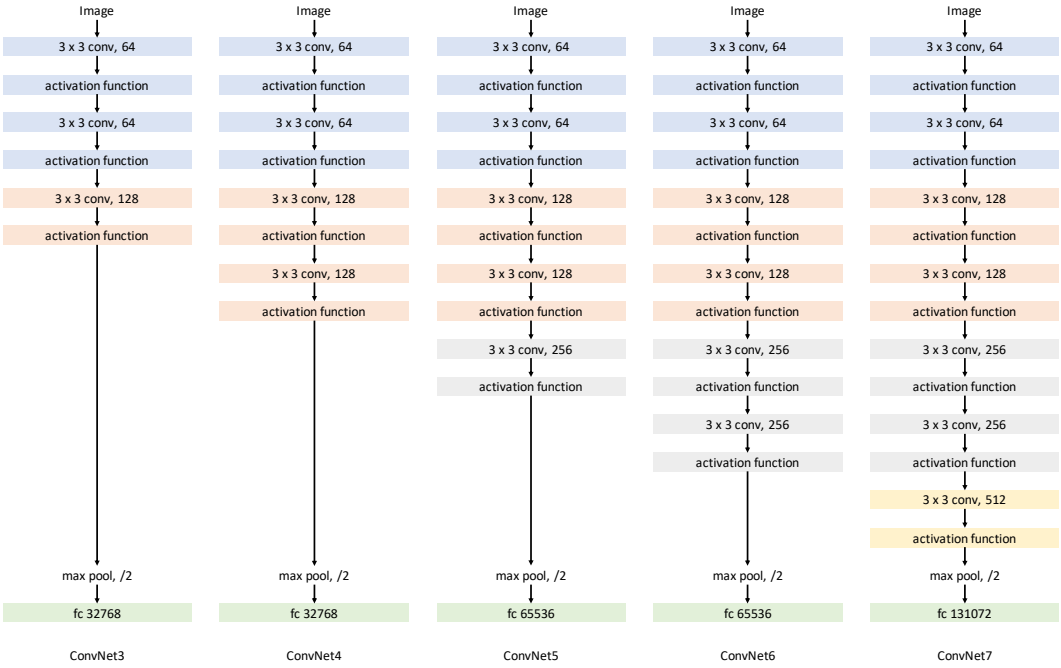

Figure 4: The architecture of `ConvNet` with different number of convolution layers.

B.2 Dataset statistics

We use both CIFAR-10 and CIFAR-100 for our experiments. As shown in Table 5, CIFAR-10 consists of 60000 images of size 32×32. It is divided into 10 classes, and each class consists of 6000 images. Also, 5000 are training data and 1000 are test data. CIFAR-100 also consists of 60000 images with a

Table 4: Setting of each convolution layer in `ConvNet`. Each version of `ConvNet` uses the number convolution layer as much as their version number. (i.e `ConvNet3` uses conv1 through conv2 and `ConvNet7` uses conv1 through conv7.)

Layer	Number of Input Filter	Number of Output Filter	Kernel Size	Padding
Conv1	3	64	3×3	1
Conv2	64	64	3×3	1
Conv3	64	128	3×3	1
Conv4	128	128	3×3	1
Conv5	128	256	3×3	1
Conv6	256	256	3×3	1
Conv7	256	512	3×3	1

size of 32×43. It is classified into 100 classes, and each class consists of 600 images. These 100 classes are divided into 20 superclasses, which we do not use in our experiments. Also, 500 are training data and 100 are test data.

Table 5: Data set statistics.

Data set	Train examples	Test examples	Class Number	Task
CIFAR-10	50,000	10,000	10	Image Classification
CIFAR-100	50,000	10,000	100	Image Classification

B.3 Training Details

In this study, we conduct numerical experiments by changing the number of clients N, the client participation ratio R, and the Dirichlet distribution constant α. We adapt FedAvg and perform 200 rounds with 5 local epochs using a learning rate of 0.01, with a learning decay of 0.1 at the 50th and 75th round, a weight decay of $1\mathrm{e}{-4}$, and a momentum of 0.9. Limited client numbers are available in different FL settings; in a *cross-silo* setting, a small number of clients are available, and a large number of clients are requested in a *cross-device*. For the *cross-silo* setting, we use $N = 20$ and $R = 0.2$ in which we select 4 clients each round. For the *cross-device* setting, we use $N = 100$ and $R = 0.2$, which we select 20 clients each round.

We mainly exhibit the training of `ConvNet4` on CIFAR-10 heterogeneously distributed by modifying the α in the Dirichlet distribution. In the captions, we explain each N, R, and α value.

C Additional Experiment Result

C.1 ConvNet4 Result

Experiment results in section 3 fix variables such as N, R, and α. Table 6 shows the result with all combinations of R and α with $N = 100$. Table 7 shows the result using CIFAR-100 with all combinations of R and α with $N = 100$. We implement all experiments on Single GPU NVIDIA 2080-Ti.

Figure 5 (a) shows the feature distribution in `ConvNet4` with different activation functions after passing the first convolution layer. After passing the convolution layer and activation function, we flatten the feature values and draw a distribution. The feature densities of the recent SOTA activation functions have discreteness and a high density near 0 due to their function shape. As the features pass deeper layers, the densities near 0 of the recent SOTA activation functions increase compared with the Tanh-like activation functions. In a centralized setting, the recent SOTA activation functions, especially ReLU work well due to its discreteness at 0 and its function shape, which is similar to a linear function which prevents the vanishing gradient and exploding gradient problems [19].

Table 6: Server accuracy of `ConvNet4` using four different α and four different participation R, where $N = 100$. The most right columns show the accuracy drop as non-IIDness increases. Since using Linear at $\alpha = 0.01, 0.1$ with participation ratio 0.1, 0.2, 0.3, and 0.4 could not train, leave blank at $\alpha = 0.01 \rightarrow 0.1, \alpha = 1 \rightarrow \alpha = 0.1$ with participation ratio 0.1, 0.2, 0.3, and 0.4.

Participation Ratio	Activation Function	$\alpha = 10$	$\alpha = 1$	$\alpha = 0.1$	$\alpha = 0.01$	$\alpha = 10 \rightarrow 1$	$\alpha = 1 \rightarrow 0.1$	$\alpha = 0.1 \rightarrow 0.01$
0.1	Linear	58.24	57.38	10.00	10.00	0.86	-	-
	Tanh	58.98	57.86	**46.61**	31.97	1.12	11.25	14.64
	HardTanh	**59.85**	**59.62**	41.90	30.34	0.23	17.72	11.56
	ReLU	51.61	49.73	41.95	28.83	1.88	7.78	13.12
	Leaky ReLU	51.60	49.76	42.05	28.90	1.84	7.71	13.15
	Swish	47.01	46.28	40.00	29.88	0.73	6.28	10.12
	Mish	50.00	49.59	43.37	**33.13**	0.41	6.22	10.24
	GeLU	48.64	48.02	41.50	31.61	0.62	6.52	9.89
0.2	Linear	62.48	62.43	10.00	10.00	0.05	-	-
	Tanh	64.49	64.14	52.58	29.50	0.35	11.56	23.08
	HardTanh	**65.27**	**65.40**	**54.43**	30.09	-0.13	10.97	24.34
	ReLU	57.80	56.23	48.37	34.03	1.57	7.86	14.34
	Leaky ReLU	57.85	56.16	48.34	33.92	1.69	7.82	14.42
	Swish	52.62	51.48	46.16	35.65	1.14	5.32	10.51
	Mish	57.30	55.08	50.02	**38.94**	2.22	5.06	11.08
	GeLU	55.59	54.34	47.46	36.09	1.25	6.91	11.37
0.3	Linear	64.66	64.46	10.00	10.00	0.20	-	-
	Tanh	67.34	66.57	**61.79**	31.35	0.77	4.78	30.44
	HardTanh	**68.35**	**67.86**	61.75	29.93	0.49	6.11	31.82
	ReLU	62.43	60.38	50.67	37.91	2.05	9.71	12.76
	Leaky ReLU	62.62	60.34	50.76	38.02	2.28	9.58	12.74
	Swish	58.04	55.88	49.45	39.78	2.16	6.43	9.67
	Mish	65.53	62.21	52.80	**42.57**	3.32	9.41	10.23
	GeLU	62.39	59.20	50.61	39.14	3.19	8.59	11.47
0.4	Linear	65.71	65.83	10.00	10.00	-0.12	-	-
	Tanh	68.83	68.37	**62.61**	29.49	0.46	5.76	33.12
	HardTanh	**69.95**	**69.35**	59.45	27.22	0.60	9.90	32.23
	ReLU	66.88	64.39	53.26	40.96	2.49	11.13	12.30
	Leaky ReLU	67.02	64.60	53.17	41.17	2.42	11.43	12.00
	Swish	64.78	60.13	51.72	41.86	4.65	8.41	9.86
	Mish	68.96	67.27	56.67	**44.41**	1.69	10.60	12.26
	GeLU	67.59	63.42	53.35	40.99	4.17	10.07	12.36

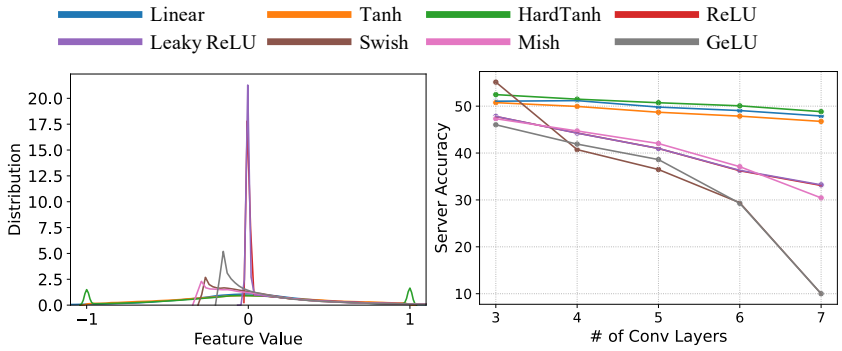

(a) Feature Distribution (b) Acc

Figure 5: (a) shows the distribution of the feature of all images of class 0 in the CIFAR-10 test dataset passing through the first convolution layer and its activation function. (b) shows the accuracy of `ConvNet` in Federated Setting with Different widths and depths. For both figure, we use $N = 100$, $R = 0.2$ and $\alpha = 0.1$.

Table 7: Server accuracy of `ConvNet4` using CIFAR-100 as dataset and $N = 100$. The most right columns show the accuracy drop as non-IIDness increases. Since using Linear at $\alpha = 0.01$ with participation ratio 0.1, 0.2, 0.3, and 0.4 could not train, leave blank at $\alpha = 0.01 \rightarrow 0.1$ with participation ratio 0.1, 0.2, 0.3, and 0.4.

Participation Ratio	Activation Function	$\alpha = 10$	$\alpha = 1$	$\alpha = 0.1$	$\alpha = 0.01$	$\alpha = 10 \rightarrow 1$	$\alpha = 1 \rightarrow 0.1$	$\alpha = 0.1 \rightarrow 0.01$
0.1	Linear	25.94	25.57	22.58	1.00	0.37	2.99	-
	Tanh	26.56	26.03	21.81	13.47	0.53	4.22	8.34
	HardTanh	**29.04**	**28.66**	**23.70**	**14.66**	0.38	4.96	9.04
	ReLU	21.83	22.67	17.98	10.97	-0.84	4.69	7.01
	Leaky ReLU	21.95	22.77	18.12	11.13	-0.82	4.65	6.99
	Swish	19.66	20.67	15.41	11.10	-1.01	5.26	4.31
	Mish	23.75	23.30	18.42	11.86	0.45	4.88	6.56
	GeLU	21.21	21.77	16.65	11.15	-0.56	5.12	5.50
0.2	Linear	31.78	31.89	28.39	1.00	-0.11	3.50	-
	Tanh	34.01	34.74	30.75	19.56	-0.73	3.99	11.19
	HardTanh	**35.68**	**36.08**	**31.76**	**21.93**	-0.40	4.32	9.83
	ReLU	26.91	27.59	23.99	15.61	-0.68	3.60	8.38
	Leaky ReLU	26.93	27.77	24.04	15.68	-0.84	3.73	8.36
	Swish	26.39	26.14	21.55	14.57	0.25	4.59	6.98
	Mish	29.40	28.89	24.89	16.41	0.51	4.00	8.48
	GeLU	27.66	26.73	23.26	15.08	0.93	3.47	8.18
0.3	Linear	35.50	35.32	31.47	1.00	0.18	3.85	-
	Tanh	37.68	38.76	34.24	23.11	-1.08	4.52	11.13
	HardTanh	**39.05**	**39.40**	**35.03**	**24.09**	-0.35	4.37	10.94
	ReLU	29.81	30.24	27.31	17.92	-0.43	2.93	9.39
	Leaky ReLU	29.74	30.26	27.45	17.97	-0.52	2.81	9.48
	Swish	29.96	29.53	25.34	17.37	0.43	4.19	7.97
	Mish	32.33	32.71	29.19	20.16	-0.38	3.52	9.03
	GeLU	30.24	29.77	27.24	17.89	0.47	2.53	9.35
0.4	Linear	37.48	37.53	33.79	1.00	-0.05	3.74	-
	Tanh	40.01	40.85	37.13	26.35	-0.84	3.72	10.78
	HardTanh	**41.69**	**41.73**	**37.41**	**27.44**	-0.04	4.32	9.97
	ReLU	30.75	31.45	30.55	20.51	-0.70	0.90	10.04
	Leaky ReLU	31.05	31.61	30.79	20.61	-0.56	0.82	10.18
	Swish	32.54	32.37	27.61	19.45	0.17	4.76	8.16
	Mish	34.64	35.94	33.11	22.01	-1.30	2.83	11.10
	GeLU	32.37	32.12	29.27	20.73	0.25	2.85	8.54

C.2 Resnet Result

Table 8, Table 9, and Table 10 shows the result of `Resnet20`, `Resnet32`, and `Resnet44` with all combinations of R and α with $N = 100$. For all values of R and α, `Resnet20` using HardTanh shows the highest accuracy. As model gets deeper, `Resnet32` and `Resnet44`, in some cases recent SOTA activation functions overcome Tanh-like activation functions. It seems to occur due to shortcut's existence. A deeper layer can use features that the activation function has excluded via a shortcut [15], which helps to prevent the recent SOTA activation functions' accuracy drop.

Table 8: Server accuracy of `Resnet20` using four different α and four different participation R, where $N = 100$. The most right columns show the accuracy drop as non-IIDness increases.

Participation Ratio	Activation Function	$\alpha = 10$	$\alpha = 1$	$\alpha = 0.1$	$\alpha = 0.01$	$\alpha = 10 \rightarrow 1$	$\alpha = 1 \rightarrow 0.1$	$\alpha = 0.1 \rightarrow 0.01$
0.1	Linear	49.01	48.60	38.60	24.63	0.41	10.00	13.97
	Tanh	50.68	49.20	38.83	23.82	1.48	10.37	15.01
	HardTanh	**51.23**	**49.44**	**39.28**	**23.91**	1.79	10.16	15.37
	ReLU	48.81	48.12	37.53	23.34	0.69	10.59	14.19
	Leaky ReLU	48.63	48.15	37.71	23.50	0.48	10.44	14.21
0.2	Linear	56.93	56.96	45.73	26.70	-0.03	11.23	19.03
	Tanh	**59.66**	57.42	**46.58**	26.50	2.24	10.84	20.08
	HardTanh	59.60	**57.54**	46.19	**26.52**	2.06	11.35	19.67
	ReLU	56.90	56.95	45.35	25.73	-0.05	11.60	19.62
	Leaky ReLU	56.78	56.49	45.18	26.10	0.29	11.31	19.08
0.3	Linear	63.17	61.67	49.35	28.25	1.50	12.32	21.07
	Tanh	**64.63**	**61.74**	49.69	**27.90**	2.89	12.05	21.79
	HardTanh	64.41	61.59	**50.16**	27.86	2.82	11.43	22.30
	ReLU	61.99	61.59	48.71	27.58	0.40	12.88	21.13
	Leaky ReLU	61.87	61.34	48.38	27.38	0.53	12.96	21.00
0.4	Linear	66.24	65.30	52.09	30.17	0.94	13.21	21.92
	Tanh	**68.08**	**65.05**	52.92	28.92	3.03	12.13	24.00
	HardTanh	67.90	64.91	**53.69**	**29.51**	2.99	11.22	24.18
	ReLU	66.10	64.94	52.54	28.28	1.16	12.40	26.26
	Leaky ReLU	66.04	64.82	52.23	28.70	1.22	12.59	23.53

Table 9: Server accuracy of `Resnet32` using four different α and four different participation R, where $N = 100$. The most right columns show the accuracy drop as non-IIDness increases.

Participation Ratio	Activation Function	$\alpha = 10$	$\alpha = 1$	$\alpha = 0.1$	$\alpha = 0.01$	$\alpha = 10 \rightarrow 1$	$\alpha = 1 \rightarrow 0.1$	$\alpha = 0.1 \rightarrow 0.01$
0.1	Linear	50.06	47.94	37.39	21.95	2.12	10.55	15.44
	Tanh	49.55	47.15	38.24	21.61	2.40	8.91	16.63
	HardTanh	50.04	47.99	**38.34**	22.37	2.05	9.65	15.97
	ReLU	50.68	48.39	37.87	**24.29**	2.29	10.52	13.58
	Leaky ReLU	**50.71**	**48.57**	37.33	23.91	2.14	11.24	13.42
0.2	Linear	60.12	56.84	43.01	24.98	3.28	13.83	18.03
	Tanh	**60.03**	56.81	43.92	25.90	3.22	12.89	18.02
	HardTanh	59.30	**57.39**	**43.99**	25.51	1.91	13.40	18.48
	ReLU	58.52	56.34	43.09	**26.66**	2.18	13.25	16.43
	Leaky ReLU	58.97	56.16	43.42	26.42	2.81	12.74	17.00
0.3	Linear	64.51	62.20	46.15	28.63	2.31	16.05	17.52
	Tanh	**64.60**	61.96	**47.77**	28.04	2.64	14.19	19.73
	HardTanh	63.74	**62.20**	47.73	28.03	1.54	14.47	19.70
	ReLU	64.23	61.58	46.49	**28.90**	2.65	15.09	17.59
	Leaky ReLU	64.20	61.59	46.81	28.49	2.61	14.78	18.32
0.4	Linear	68.45	65.75	49.49	30.28	2.70	16.26	19.21
	Tanh	**67.75**	**66.58**	**51.03**	29.41	1.17	15.55	21.62
	HardTanh	67.33	66.17	50.75	29.18	1.16	15.42	21.57
	ReLU	67.52	65.55	49.72	30.18	1.97	15.83	19.54
	Leaky ReLU	67.46	65.71	49.40	**30.43**	1.75	16.31	18.97

Table 10: Server accuracy of `Resnet44` using four different α and four different participation R, where $N = 100$. The most right columns show the accuracy drop as non-IIDness decreases.

Participation Ratio	Activation Function	$\alpha = 10$	$\alpha = 1$	$\alpha = 0.1$	$\alpha = 0.01$	$\alpha = 10 \rightarrow 1$	$\alpha = 1 \rightarrow 0.1$	$\alpha = 0.1 \rightarrow 0.01$
0.1	Linear	49.68	47.28	39.56	23.26	2.40	7.72	16.30
	Tanh	49.13	46.47	38.19	23.06	2.66	8.28	15.13
	HardTanh	**49.33**	**47.10**	**38.88**	**23.77**	2.23	8.22	15.11
	ReLU	48.89	46.38	38.57	22.84	2.51	17.81	15.73
	Leaky ReLU	48.77	46.27	37.35	23.05	2.50	8.92	14.30
0.2	Linear	57.55	55.98	45.14	27.50	1.57	10.84	17.64
	Tanh	57.94	55.54	**46.42**	**27.23**	2.40	9.12	19.19
	HardTanh	**58.80**	**57.54**	45.98	26.46	1.26	11.56	19.52
	ReLU	56.89	54.23	44.42	26.06	2.66	9.81	18.36
	Leaky ReLU	57.02	53.76	43.97	26.37	3.26	9.79	17.60
0.3	Linear	63.29	61.20	47.78	30.71	2.09	13.42	17.07
	Tanh	**64.43**	61.27	50.67	**29.53**	3.16	10.60	21.14
	HardTanh	64.31	**61.42**	**51.23**	28.84	2.89	10.19	22.39
	ReLU	62.79	60.19	46.25	28.41	2.60	13.94	17.84
	Leaky ReLU	62.63	59.63	46.84	28.27	3.00	12.79	18.57
0.4	Linear	67.30	65.09	51.25	32.67	2.21	13.84	18.58
	Tanh	**68.14**	64.67	52.89	**32.37**	3.47	11.78	20.52
	HardTanh	67.91	**65.02**	**53.95**	31.90	2.89	11.07	22.05
	ReLU	66.74	64.20	50.31	30.51	2.54	13.89	19.80
	Leaky ReLU	66.41	64.26	50.40	31.03	2.15	13.86	19.37

C.3 MobileNetv2 Result

Table 11 shows the result of `MobileNetv2` with four different R with $N = 100$ and $\alpha = 0.1$. Tanh-like activation functions surpass recent SOTA activation functions. Especially recent SOTA activation functions accuracy is lower than Linear.

Table 11: Server accuracy of `MobileNetv2` with four different participation ratio R (0.1, 0.2, 0.3, 0.4). We use $N = 100$ with $\alpha = 0.1$.

Activation Function	CIFAR-10				CIFAR-100			
	$R = 0.4$	$R = 0.3$	$R = 0.2$	$R = 0.1$	$R = 0.4$	$R = 0.3$	$R = 0.2$	$R = 0.1$
Linear	36.74	36.86	35.86	35.50	15.02	14.76	14.23	13.17
Tanh	33.39	33.64	**31.59**	**31.83**	**19.20**	**16.99**	**14.76**	**11.19**
HardTanh	33.82	32.41	28.91	29.95	18.64	15.91	13.54	9.39
ReLU	**36.99**	**34.21**	26.93	20.12	16.71	13.97	8.16	5.17
Leaky ReLU	35.54	33.07	30.69	20.44	16.92	13.84	10.14	5.67

C.4 FedProx Result

As mentioned in section 1, studies to improve the server model in FL add proximal terms to the local object to enhance the method's stability so that the local model rarely differs from the global model. We choose FedProx [33] as an additional FL method because it is the most basic method that focuses on improving the server model by adding a proximal term. The details of FedProx is shown in Appendix B. Table 12 shows the accuracy for different activation functions using FedProx as a learning algorithm. Similar to FedAvg, HardTanh achieves the best accuracy, followed by the other Tanh-like activation functions. Proximal terms in local training do not appear to help prevent accuracy loss.

Table 12: Server accuracy using FedProx with following setting: $N = 100$, $R = 0.2$, and $\alpha = 0.1$.

Act. Func.	Acc.
Linear	48.74
Tanh	45.50
HardTanh	**49.16**
ReLU	42.19
Leaky ReLU	42.40
Swish	35.79
Mish	39.83
GeLU	36.00

D Landscape Result

We visualize the affect of different activation functions; Tanh, HardTanh, ReLU, and Leaky ReLU. The color bar beside each figure shows the loss difference. Tanh and HardTanh has extremely small number compared to ReLU and Leaky ReLU. Which emphasize that Tanh and HardTanh smooth out the landscape considerably comparison to ReLU and Leaky ReLU. Additionally, Tanh and HardTanh has its significant lowest value where perturbation X and perturbation Y is both 0. However, ReLU and Leaky ReLU does not show this phenomenon. Which we can consider that only Tanh and HardTanh succeed in reaching the global optimum.

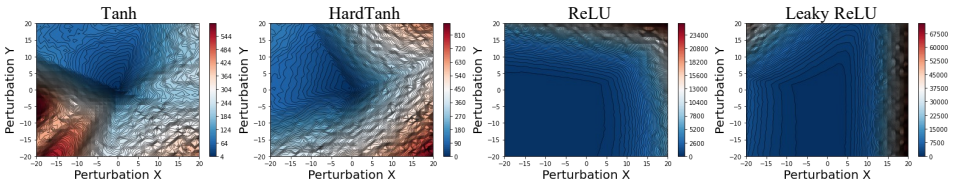

Figure 6: Landscape of `ConvNet4` with Tanh, HardTanh, ReLU and Leaky ReLU. We use $N = 100$ with $R = 0.1$ and $\alpha = 0.01$ for training. We draw landscape with 150 levels.